SCIENCE CHINA
Technological Sciences

April 2012 Vol.55 No.4: 1132–1139
doi: 10.1007/s11431-011-4721-5

Calculation model of AC loss for CICC (cable-in-conduit conductor) based on strain

JIANG HuaWei[1*], WU SongTao[2], ZHANG DeXian[1], XU ZhaoHui[1] & ZHEN Tong[1]

[1] *College of Information Science and Engineering, Henan University of Technology, Zhengzhou 450001, China;*
[2] *Institute of Plasma Physics, Chinese Academy of Sciences, Hefei 230031, China*

Received August 22, 2011; accepted December 9, 2011; published online February 25, 2012

The CICC (cable-in-conduit conductor) in ITER (International Thermal-nuclear Experimental Reactor) will run in high-current, fast transient magnet field and complex environment. In response to the impact of magnet fields above 10 T, the Nb_3Sn conductor has been introduced. However, the AC (alternating current) loss mechanism of Nb_3Sn conductor on strain has not been explored. So, it is necessary to study the AC loss calculation method with transient electromagnetic field and wide range of strain, the coupling current in complex field and current signal of field is simplified to the spectrum effects of coil excitation, and calculation technology of AC loss, which contains the frequency, magnet field, coil characteristics and other parameters, is constructed to meet the discrete Fourier transform (DFT). By comparative analysis of simulation, it is found that the AC loss calculation of the conductor with spectrum algorithm is closer to the actual project value than the traditional algorithm. For the rapid excitation, in particular plasma discharge and burst, spectrum algorithm and the traditional algorithm are consistent. For the relative error calculation of hysteresis loss and coupling loss, it is found that the coupling loss is cumulative linearly, where the hysteresis loss is not so. As a function of the amplitude, frequency and phase angle, the relative error is less than 40%. The results showed that the method of Fourier restructuring is satisfactory.

cable-in-conduit conductor (CICC), strain, numeric simulation, AC loss, calculation model

Citation: Jiang H W, Wu S T, Zhang D X, et al. Calculation model of AC loss for CICC (cable-in-conduit conductor) based on strain. Sci China Tech Sci, 2012, 55: 1132–1139, doi: 10.1007/s11431-011-4721-5

1 Introduction

The cable-in-conduit conductor (CICC), which is based on the concept of CIC (cable in conduit) by Chester, Altov and Hoenig, evolved from the internally-cooled superconductor (ICS) [1, 2]. With the rapid development of superconducting theory and engineering application, the CICC with the advantages of supercritical helium cooling, high voltage insulation, low AC loss and multistage cabling, has been selected as the preferred conductor for use to Toroidal Fields (TFs), Poloidal Fields (PFs) in Experimental Advanced Superconducting Tokamak (EAST, in China), Korean Superconducting Tokamak Advanced Research (KSTAR) and International Thermal-nuclear Experimental Reactor (ITER). Moreover, the CICC is one of the important conductors in the hybrid high magnet field.

The CICC of the EAST superconducting Tokamak device which was constructed in China adopted the technology of NbTi and pure copper strands [3]. However, the conductor of ITER, which will run in the complicated electromagnetic environment, should be subjected to impacting more than 10 T. Because of limitation of the NbTi-based CICC critical performance, it is difficult to meet operation requirements. All the CSs, TFs and part of PFs in ITER will use the Nb_3Sn-based CICC, which has been developed based on niobium titanium (NbTi) technology. And yet, the

*Corresponding author (email: lhwcad@sohu.com)

strain caused by heat, mechanical and other factors is a key problem that is widely observed. It is a response to the spread and dissemination of heat energy in a CICC, and gives rise to the quench phenomenon. It is obvious that strain will affect the operation of a CICC, and it is important in engineering design to carry out research of stability theory under the strain effect of the Nb_3Sn-based CICC.

So far, there has been some progress in the theoretical investigation on these problems. For example, degradations of Nb_3Sn conductors for the ITER model coils were found in 2002 and 2006 [4], the strain caused by electric force brings the internal bending of the CICC and performance degradation, and gives the thought to improve processing and testing methods. Wu's team [5, 6], Zhang's team [7, 8], Wang's team [9] and other teams carried out a lot of experimental analyses on the conductor of ITER with Nb_3Sn strand and short sample of the CICC, analyzed the sensitivity of critical current density to different strain and deterioration, and proposed to improve the performance of the critical current through controlling strain.

In addition, the Nb_3Sn conductor, in the fast changing magnet field by excitation current, will be sustained by the AC (alternating current) loss different from NbTi. Based on the AC loss calculation method of NbTi, a lot of work on AC loss calculation of Nb_3Sn has been explored [2, 10−12]. For the low-frequency and slow changing magnet field, the AC loss calculation model of ITER CICC is proposed [13], where the AC loss is disposaled by dividing it into three-dimensional complex scalar. For the uniform time-varying transverse magnet field, coupling loss calculation technique of the CICC is given [14], the induced current in pair between sub-cables is treated, including pair of superconducting strands and copper strands. Because these calculation models contain a large number of coil geometries, the real-time magnet field and the spatial location of the coil need to be generated and determined, the traditional AC loss calculation is much complicated and not suitable for the optimization of fast-changing field.

With the project on the numerical study of the CICC based stability [15], and the proposed numerical simulation model of the CICC to obtain the optimized and reasonable structure of the conductor with multi-variable constraints [16] and other preliminary work, it is found that the AC loss calculation of the NbTi-based CICC is lack of the study of the AC loss for the Nb_3Sn conductors under the strain influence. With the grain specific defects, the void fraction, spatial location and contact status of the Nb_3Sn conductors caused by residual stress will change, and will lead to the distortion of pinning force and the coupling loss time constant. In the end, it will result in unpredictable change for the hysteresis loss and coupling loss. Therefore, the mechanism of AC loss for the Nb_3Sn conductor needs to be studied under the strain effect. In this paper, the transformation of magnet field and the excitation current signal spectrum are first discussed, the discrete Fourier transform (DFT) is then built, and the simplified calculation theory of the coupling loss is finally proposed, which considers the frequency (the excitation current to produce spectrum is related to critical current, whereas the critical properties of Nb_3Sn, especially critical current, is affected by the strain (see Section 2.1), field strength and coil characteristics (it is related to the strain effect, see Section 2.1). By these studies, the theory of complex dynamic AC loss in the alternating magnet field and the stable operation mechanism of the Nb_3Sn conductor are understood clearly under the conditions of fast excitation and plasma burst.

2 Traditional calculation model of AC loss

2.1 Theoretic basis of AC loss

A CICC, in fast time-varying magnet field or current (excitation coil), performs differently from the DC. It will produce AC loss, including both hysteresis loss and coupling loss.

Hysteresis loss is energy consumption, which works to drive flux lines movement and overcome pinning force. For Nb_3Sn conductor, its pinning center is mainly formed by grain boundaries. So, the diffusion reaction and special heat treatment process is needed in manufacturing of superconductor. The strain resulting from low temperature operation and Lorentz force will affect the critical parameter, especially for the pinning force. With the strain effect, the coupling loss calculation of the Nb_3Sn conductor is different from that of the NbTi.

Coupling loss is also energy consumption, which is caused by the induced current flowing between the superconducting filaments and resistant matrix, it exists in all superconducting cables. The void fraction of the Nb_3Sn-based CICC and contact status will change with strain resulting from heat treatment and low temperature operation, it will cause unpredictable change for the calculation of coupling loss time constant. Therefore, the coupling loss calculation is different from that of NbTi.

2.2 Calculation model of hysteresis loss

Hysteresis loss can be calculated by the power of Lorentz force, which can be obtained by integral with magnetization curve of superconductors in changing magnet field, it also can be gained by integral with Poynting vector $S=E\times H$ to current or field, as well as by dot metrix integral of the conductor current density j and electric field E.

The hysteresis loss per unit volume can be obtained by experience and theoretical analysis [17].

$$W_{\mathrm{p}} = \frac{1}{6} J_{\mathrm{C}} d_{\mathrm{e}} A_{\mathrm{SC}} \dot{B}, \tag{1}$$

where J_{C} is the critical current density, d_{e} is the effective radius of superconducting wire, A_{SC} is the total cross section

of superconducting wire in the cable, $\dot{B}$ is the change rate of the magnet field

The hysteresis loss can be obtained by volume integral with hysteresis loss power above.

$$W = \int_V W_{\mathrm{p}} \mathrm{d}v. \tag{2}$$

2.3 Calculation model of coupling loss

The superconducting cable is twisted with multi-strands, and all of the strands are full transposition. For coupling loss calculation, the effective transverse resistivity and the effective torque are different from those of strands. In order to get the suitable formula for coupling loss calculation of superconducting cable, by the simplified method, the higher accuracy formula to calculate the coupling loss of the CICC can be achieved.

In the process of calculation, the coil excitation (PF) and the stability characteristics of the CICC need to be considered. Under the extreme condition of plasma discharge or burst, the superconducting wires in the CICC are almost saturated. Taking into account the saturation coefficient, the coupling loss of the CICC can be calculated as follows [15]:

$$P = \begin{cases} \dfrac{2\theta}{u_0} \dot{B}_{\mathrm{T}}^2 (1-\beta), & \beta < 0.31; \\ \dfrac{4}{3\pi} \dfrac{B_{\mathrm{P}}}{u_0} \dot{B}_{\mathrm{T}}, & \beta \geqslant 0.31; \end{cases} \tag{3}$$

where θ is the coupling loss time constant, B_{T} is the transverse magnet field, β is the saturation coefficient, B_{p} is the penetration field, and u_0 is the magnetic permeability of vacuum.

It is obvious that the coupling loss time constant is the main parameter, and can be calculated by the following formula:

$$\theta = \sum_{n=1}^{N} \theta_n, \tag{4}$$

where θ_n is the addition of coupling loss time constant of the nth level, it can be expressed as follows:

$$\theta_n = \frac{\mu_0}{2\rho_n} \left(\frac{P_n^*}{2\pi} \right)^2 \frac{1}{1 - f_{vn-1}}, \tag{5}$$

where P_n^*, ρ_n and f_{vn} are the effective length, the effective resistivity and void fraction of the nth level, respectively.

The effective length and the effective resistivity can be written in eqs. (6) and (7) below.

$$P_n^* = P_n - \frac{r_{n-1}}{R_{n-1}} P_{n-1}, \tag{6}$$

$$\rho_n = \frac{\rho_{\mathrm{b}} e_{\mathrm{b}}}{M_n R_{n-1}}, \tag{7}$$

where P_n, R_n, r_n and M_n are the length, the radius, the radius of wire and the ratio of the contact surface of the nth level, respectively; $\rho_{\mathrm{b}} e_{\mathrm{b}}$ is the character of contact resistance.

Especially, when n =2, r_1 is the radius of the wire, and R_1 is the radius of the strand.

2.4 Ratio of the contact surface

The ratio of the contact surface in the above formula is the key parameters to affect the coupling loss calculation. So the experience formula needs to be studied. For the CICC conductor, the ratio of the contact surface can be expressed as follows [18]:

$$M_n = \frac{R_n}{R_{n-1}} M_{n-1}, \tag{8}$$

where R_n is the radius of the nth subcable. In the range of the void fraction between 0.28 and 0.4, it can be known that the ratio of area contact increases as the radius of the twisted cable decreases.

3 Spectrum calculation model of AC loss

3.1 Basic conception model

In the complicated magnet field, according to ref. [19], taking into account the strain effect of the Nb_3Sn conductor, the excitation current is taken between 1/2 and 2/3 of the critical current, the strain effect quantitative model on critical current of Nb_3Sn conductor is drawn from ref. [20] (which is similar to the relationship between critical current density and n-value in the HTS tapes [21]). Based on the strain effect, the simplified results of excitation current can be obtained.

In the spectrum calculation model, the theory analysis of discrete Fourier transform (DFT) matrix for solving the different excitation current signals of the CICC is explored. The transform of Fourier components from the vector to the scalar is analyzed. Moreover, the AC loss components calculation method of the CICC, which contains the magnet field, the frequency and the characteristics of conductor, is built. The calculation technology of the AC loss is achieved.

By taking into account the strain effect, the coupling current of the Nb_3Sn-based CICC and the penetration field are simplified to the spectrum effects of coil excitation. DFT, which is used to generate the spectrum of the CICC by excitation current, is constructed. Moreover, the frequency domain analysis is carried out.

Each Fourier component of the excitation current can be changed into the vector by the effective transformation matrix function, where the main task is to get the superposition of all vector field contributions in conductor by the excitation coil.

It is the key technology to complete the conversion from

the vector to scalar in the model. A series of variables expressions can be obtained with the magnet field, frequency and characteristics of the conductor, which contains the void fraction of the CICC, the effective torque, the effective wire diameter, and the characterization of surface contact for each level cable and the coupling loss time constant. According to these concept and analysis, the AC loss components can be calculated. In the actual measurement, due to the impact of strain, there is some difference for the same structure of the Nb_3Sn and NbTi based CICC in their void fractions and characterization of surface contact.

Based on mathematical expression of loss, the total loss of the CICC can be summed linearly by the different loss components of excitation current corresponding to frequency.

3.2 Calculation model of spectrum

In order to simplify the calculation model and to obtain reasonable results, some of the limits and assumptions are given as follows: ① In a given position, the excitation field that leads to loss power density of the CICC is a periodic function. ② In a given position, the relationship between the contributions of magnet field caused by excitation coil is linear; ③ The loss contribution of each coil is increased linearly. ④ The parameters of the CICC (such as cross section of cable, length, wire diameter) are constant.

According to condition ①, the AC loss of the CICC can be calculated by integral of power density $\dot{q}_f(B(x,f),x,f)$ at position x with frequency f.

$$q_f = \int_t \int_{V_i} \dot{q}_f(B(x,f),x,f)\mathrm{d}x\mathrm{d}t, \tag{9}$$

where V_i is the coil volume. In the ITER magnetic system, the magnet field is only generated by the currents and ferromagnetism contribution, the contribution of diamagnetism materials can be ignored. By condition ②, the magnet field is superposition linear. Fourier transform operation can be expressed as follows:

$$\tilde{\boldsymbol{B}}_j(x,f) = \sum_j \boldsymbol{T}_j(\mathrm{x})\tilde{\boldsymbol{I}}_j(f), \tag{10}$$

where $\boldsymbol{T}_j(x)$ is the transformation matrix.

The Fourier components of the current spectrum can be written as

$$\tilde{\boldsymbol{I}}_j(f) = \boldsymbol{F}[I(t)], \tag{11}$$

where $\boldsymbol{F}[]$ is the vector format of Fourier component, the overall system energy formed by the contribution of real and imaginary parts, i.e. amplitude and phase.

As ③ shows that the loss of the CICC can be obtained by integral of power density in entire coil volume. The loss can be written by all frequency contributions with DFT.

$$q_f \approx \sum_k \int_{V_i} \dot{q}_f(B(x,f),x,f)\mathrm{d}x. \tag{12}$$

The power density of loss is the location function of the excitation field with frequency f, it can be expressed with the background field, change field and the parameters of the CICC.

$$\dot{q}_f(B(x,f),x,f) = \psi[B_0(x),\Delta B(x,f),f,C_i] \tag{13}$$

where $B_0(x)$ is the background field (constant), $\Delta B(x, f)$ is the amplitude of change field with frequency f, representing a calculation sequence of discrete Fourier components. C_i is a series of the AC loss calculation parameters, such as cross section of cable, length of cable, time constant, magnetization factor, wire diameter and the critical current. $\psi[]$ is the loss function of the mean field, it depends on the common expression of vector field components, which contains a number of the real components (hysteresis loss and coupling loss)

If vector module is used instead of the vector field, the background field will become Fourier components with zero frequency.

$$B_0(x) = \left|\mathrm{Mod}\left[\sum_j \boldsymbol{T}_j(x)\tilde{\boldsymbol{I}}_j(0)\right]\right|, \tag{14}$$

where Mod[·] is the operation module to produce the composite number (to reduce information of the phase), |·| is the operation module of the 3D vector (to reduce information of space direction) .

Similarly, the amplitude of change field can be expressed as follows:

$$\Delta B(x,f) = \left|\mathrm{Mod}\left[\sum_j \boldsymbol{T}_j(x)\tilde{\boldsymbol{I}}_j(f)\right]\right|. \tag{15}$$

The loss equation can be gotten as follows:

$$q_f \approx \sum_k \int_{V_i} \psi\left[\left|\mathrm{Mod}\left[\sum_j \boldsymbol{T}_j(x)\tilde{\boldsymbol{I}}_j(0)\right]\right|, \left|\mathrm{Mod}\left[\sum_j \boldsymbol{T}_j(x)\tilde{\boldsymbol{I}}_j(f)\right]\right|, f, C_i\right]\mathrm{d}x. \tag{16}$$

As ③ shows that the total AC loss can be summed by the loss of all components (linear component), it can be written in the following integral form:

$$q_f \approx V_i \sum_l \sum_k \int_{V_i} \psi\left[\left|\mathrm{Mod}\left[\sum_j \boldsymbol{T}_j(x)\tilde{\boldsymbol{I}}_j(0)\right]\right|, \left|\mathrm{Mod}\left[\sum_j \boldsymbol{T}_j(x)\tilde{\boldsymbol{I}}_j(f)\right]\right|, f, C_i\right]\mathrm{d}x. \tag{17}$$

The above formula contains a large number of complexity parameters with volume integral. Using condition ④, that is, the parameters of the conductor are constant, combining with the background field (obtained by mean-field module in the whole CICC space) and changing magnet field (obtained by given frequency module), the estimates of the AC loss can be obtained by integral of mean-field loss

function ψ[] in the volume.

$$q_f \approx V_i \sum_l \sum_k \psi \left[\left| \mathrm{Mod}\left[\sum_j \bar{\boldsymbol{T}}_{ij} \tilde{\boldsymbol{I}}_j(0) \right] \right|, \left| \mathrm{Mod}\left[\sum_j \theta_{jl} \bar{\boldsymbol{T}}_{ij} \tilde{\boldsymbol{I}}_j(f) \right] \right|, f, C_i \right]. \quad (18)$$

where θ_{jl} is the weight factor, which is the transformation function of each component caused by the *j*th excitation coil. It can be obtained by the least squares fit. $\bar{\boldsymbol{T}}_{ij}$ is the average volume transformation function of the CICC for the *j*th excitation coil. It is expressed as follows:

$$\bar{\boldsymbol{T}}_{ij} = \frac{1}{V_i} \int_{V_i} \boldsymbol{T}_j(x) \mathrm{d}x. \quad (19)$$

The background field B_0 can be obtained by mean-field module in the whole CICC space.

$$B_0(x) = \frac{1}{V_i} \int_{V_i} \left| \mathrm{Mod}\left[\sum_j \boldsymbol{T}_j(x) \tilde{\boldsymbol{I}}_j(0) \right] \right| \mathrm{d}x = \left| \mathrm{Mod}\left[\sum_j \left(\frac{1}{V_i} \int_{V_i} \boldsymbol{T}_j(x) \mathrm{d}x \right) \tilde{\boldsymbol{I}}_j(0) \right] \right|. \quad (20)$$

Similarly, the amplitude of magnet field can be obtained by the given frequency.

$$\Delta B(x,f) = \frac{\theta_{jl}}{V_i} \int_{V_i} \left| \mathrm{Mod}\left[\sum_j \boldsymbol{T}_j(x) \tilde{\boldsymbol{I}}_j(f) \right] \right| \mathrm{d}x = \left| \mathrm{Mod}\left[\sum_j \left(\frac{\theta_{jl}}{V_i} \int_{V_i} \boldsymbol{T}_j(x) \mathrm{d}x \right) \tilde{\boldsymbol{I}}_j(f) \right] \right|. \quad (21)$$

4 Results and discussion

4.1 Experiment conditions

In order to fit and simplify the AC loss calculation model of the CICC in ITER, the period function of magnet field is selected with frequency *f* (such as the sine function form), whose maximum field and the smallest field are $B_{\max}$ and $B_{\min}$, respectively.

When the change magnet field is greater than the mean field, the smallest field becomes negative. In order to simplify the AC loss calculation of two parts in the period, the part between 0 and $B_{\max}$ is positive field, and the other part between $B_{\min}$ and 0 is negative field (as indicated in Figure 1). Dealing with two parts separately and adding energy of each cycle, the accurate AC loss in entire cycle can be obtained.

The CICC structure of TFMC (toroidal field model coil) for the ITER magnet system is shown as Figure 2, which is made from Nb_3Sn. From Figure 2 we can see the configuration of the CICC. The first sub-cable contains three superconducting strands, the second sub-cable is made of 3 first sub-cables, in the third sub-cable there are 5 second sub-cables, the fourth sub-cable includes 4 third sub-cables, and 6 fourth sub-cables form the cable. Finally, the cable that was embedded in the stainless steel conduit was transfigured into squared shape.

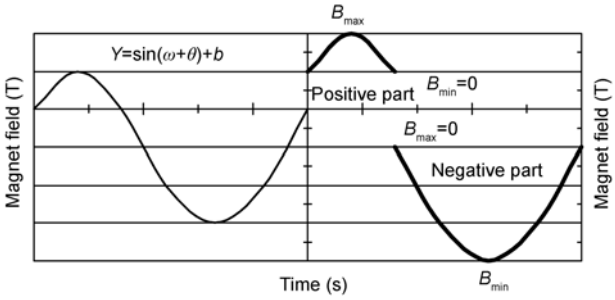

Figure 1 Schematic diagram of the magnetic field.

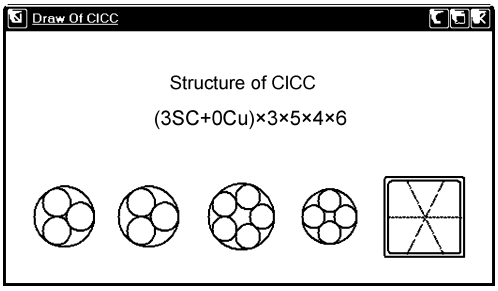

Figure 2 Structure of CICC.

4.2 AC loss calculation of CICC in ITER

For the AC loss calculation of the CICC in ITER magnet system, assuming that the background field is superposition of harmonic excitation, the parameters model is established by the above description. In the model there are 13 concentric solenoid coils, including central solenoid coils (CS1-CS6), PF coils (PF1-PF6) and plasma produced in vacuum chamber.

In the model, it is key to calculate all component contributions of the coils in the magnet field. The background field caused by the *j*th coil at the position *x* in the CICC can be calculated in the following expression:

$$B_0(x,t) \approx \sum_{j=1}^{N_{\mathrm{coils}}} \boldsymbol{T}_j(x) I_j(t), \quad (22)$$

where N_{coils} is the number of coils (it is 13 in the model).

According to the magnet field of the solenoid, the average background field of harmonic excitation can be calculated as follows:

$$\bar{B}_0(t) = \frac{1}{V_1} \int_{V_1} |B(x,t)| \mathrm{d}x = \frac{1}{V_1} \int_{V_1} \left| \sum_{j=1}^{N_{\mathrm{coils}}} \boldsymbol{T}_j(x) I_j(t) \right| \mathrm{d}x. \quad (23)$$

The background field of the CICC was only produced by the *j*th coil. Once the background field is gotten, the change field ΔB_j of the CICC can be obtained with eq. (24), which is produced by current changing and linear superposition of the *j*th coil.

$$\Delta B_j = \frac{\theta_j}{V_i}\int_{V_i} |\boldsymbol{T}_j(x)|\mathrm{d}x\Delta I_j = \theta_j \overline{\boldsymbol{T}}_{ij}\,\Delta I_j. \tag{24}$$

The weight factor θ_j is related to change of mean field for the AC loss calculation. In the expression of loss, especially for the case that the hysteresis loss is not always linear, the average magnet field power will be considered.

There are two methods to calculate AC loss. The first one is the spectrum algorithm, where the total AC loss can be obtained by calculating each harmonic field and cumulating contribution of each frequency with the formulas in Section 2.2. The second one is traditional algorithm in Sections 1.2 and 1.3. The hysteresis loss and coupling loss also can be obtained by integral with instantaneous loss power. The hysteresis loss power can be expressed as follows:

$$q_{\mathrm{H}} = \frac{2}{3\pi} J_{\mathrm{C}} d_{\mathrm{e}} \left|\frac{\mathrm{d}B}{\mathrm{d}t}\right|. \tag{25}$$

The expression of the coupling loss and total loss can be written in eqs. (26) and (27).

$$q_{\mathrm{C}} = \frac{\theta}{\mu_0}\left(\frac{\mathrm{d}B}{\mathrm{d}t}\right)^2, \tag{26}$$

$$q_{\mathrm{P}} = q_{\mathrm{H}} + q_{\mathrm{C}}. \tag{27}$$

The AC loss calculation of the spectrum algorithm and the traditional algorithm is shown in Figure 3.

From Figure 3, it can be seen that the value of the AC loss power with spectrum algorithm is smaller than that of traditional algorithm. In general, the value of the AC loss power by the experimental measurements is smaller than that of traditional algorithm. Therefore, the spectrum algorithm value is close to the engineering value. In the case of low frequency, there is an obvious difference between the traditional algorithm and spectrum algorithm. However, at high frequency, for the fast excitation, especially plasma discharge and burst, the spectrum algorithm and the traditional algorithm are consistent.

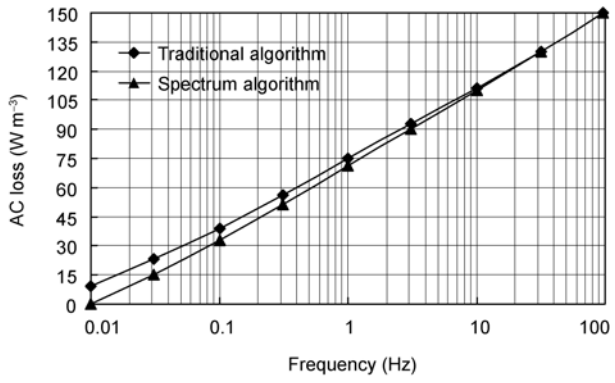

Figure 3 Comparison of AC loss with two algorithms.

4.3 Relative error calculation and analysis of Fourier component with simple field

Based on the above calculation, the error evaluation of the AC loss is given with the simple spectrum components by Fourier component linear superposition for the purpose of the expected error limits being given in the worst case.

For the measurement and analysis, the field perpendicular to the conductor is adopted by eq. (28):

$$B = \frac{\Delta B_1}{2}\sin(2\pi f_1 t) + \frac{\Delta B_2}{2}\sin(2\pi f_2 t + \varphi). \tag{28}$$

It is composed of two harmonic functions, whose amplitude is arbitrary. However, the frequency ratio f_1/f_2 is an integer, and the cycle integer multiple of the smaller frequency is their period. For the given frequency, the coefficient of DFT is equal to $\Delta B_1/2$ or $\Delta B_2^2/2$. The relationship between the spectrum signal and its discrete Fourier transform is shown in Figure 4.

For solving the relationship of DFT with the different frequencies, it is required to obtain the desired amplitude of magnet field with algebraic addition and subtraction, by which the overlay spectrum can be produced.

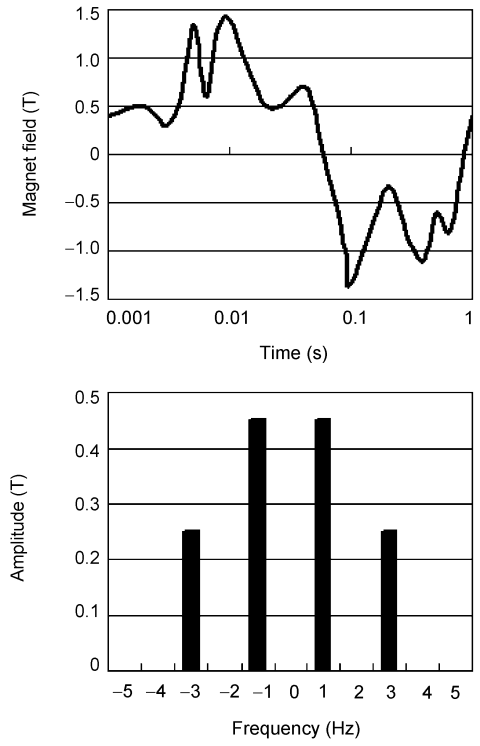

Figure 4 DFT of simple field and the frequency of the signal.

The experimental data, in a relatively wide parameters area of amplitude, frequency and the phase angle, are analyzed. According to the changes of harmonic excitation field ratio and frequency ratio and phase angle, the error is discussed,

The relative error is expressed as follows with discrete Fourier components by the spectrum formula and the traditional formula.

$$\text{Error} = \frac{q_{\text{P}} - q_f}{q_f}. \tag{29}$$

For the hysteresis loss and coupling loss, it is found that the relative error of coupling loss is cumulative linearly, where the shielding effect is ignored. Estimate of each component is equal to the sum of all signals corresponding to the time integral of power, which directly results from Fourier series features. It is conserved for energy in domain of time and frequency

For the hysteresis loss, it is not always linear. When frequency ratio f_1/f_2=2 and phase angle φ=0° or φ=90°, the relative error ratio changing with the harmonic field amplitude is shown in Figure 5. It can be seen that hysteresis loss was estimated better for the larger or smaller amplitude ratio. For the middle of the amplitude ratio, in particular, 0.1 $<\Delta B_1/\Delta B_2<$10, the relative error is larger (hysteresis loss is overestimated by Fourier restructuring). When the phase angle is 90°, the worst case appears, where the peak of relative error is about 40%.

The relative error as the function of the phase angle is shown in Figure 6. When the amplitude ratio $\Delta B_1/\Delta B_2$= 0.75 and frequency ratio f_1/f_2=1, the relative error fluctuates between 20% and 35%. It can be observed that the relative error is affected by the phase angle. In this range, the difference of the relative error is relatively small, which is less than 15%.

The impact of harmonic frequency is shown in Figure 7. Given the condition of $\Delta B_1/\Delta B_2$=0.75 and difference of phase angle is 90°, the relative error becomes the function of frequency ratio in the range of 0.1–10. In this region, the relative error decreases with the increase of the frequency ratio. For the large frequency ratio, the component characteristics of loss can be distinguished clearly. So, the satisfactory results of Fourier restructuring can be gotten.

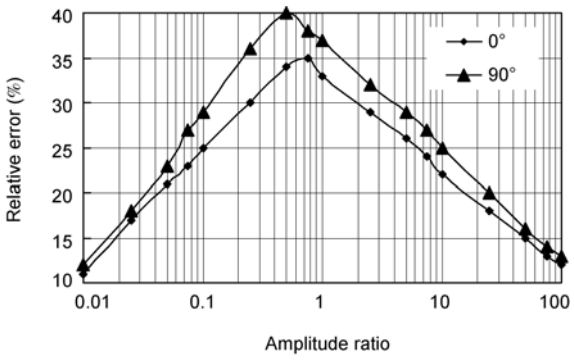

Figure 5 Relative error changes with amplitude ratio

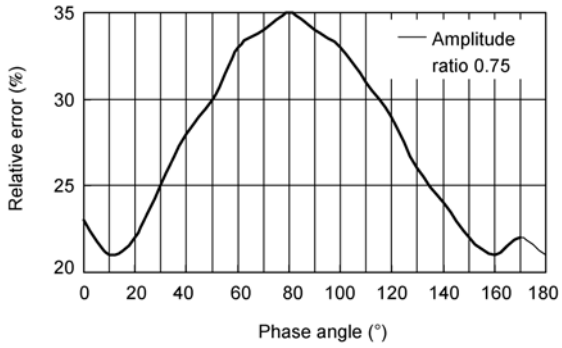

Figure 6 Relative error changes with phase angle.

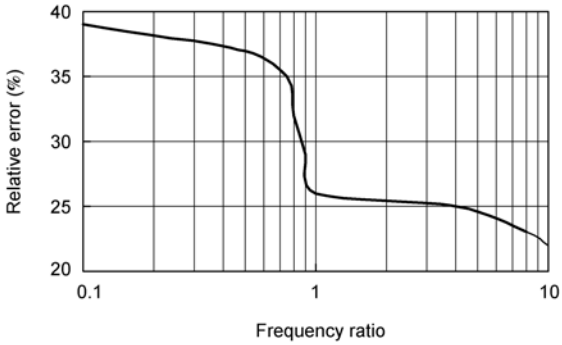

Figure 7 Relative error changes with frequency ratio.

5 Conclusion

By the simplified model of the AC loss calculation, a quick estimating AC loss method of the CICC in ITER magnet system is put forward, which can obtain the total AC loss based on calculation of each component with Fourier decomposition in the excitation magnet field and all frequency contributions associated with the given current.

By the analysis of simulation, it is found that the AC loss calculation of the CICC with spectrum algorithm is close to the actual project value. For the case of low frequencies, there is a large difference between spectrum algorithm and traditional algorithm. For the fast excitation, especially plasma discharge and burst, the spectrum algorithm and the traditional algorithm are consistent.

For the relative error calculation of hysteresis loss and coupling loss, it is found that the coupling loss is cumulative linearly, and the hysteresis loss is not entirely so. The relative error changes with the amplitude ratio, and is less than 40%. The relative error, as function of phase angle, is fluctuates between 20% and 35%. The relative error decreases with the increase of the frequency ratio, for the larger frequency ratio, the satisfactory results of Fourier restructuring can be gotten.

The method to estimate the AC loss of the CICC can be quickly gotten based on the analysis expression of Fourier restructuring in the excitation field. In the model, the AC loss calculation is related to calibration of amplitude and frequency. The method not only can better estimate the total AC loss, but also can analyze the contribution of each component in the conductor, and the model can optimize and control the plasma position and shape rapidly.

This work was supported by the Major International (Regional) Joint Research Program of China (Grant No. 2004CB720704) and the Excellent Young Teachers Program for Higher Education of Henan Province (Grant No. 2010GGJS-088).

1 Dresener L. Twenty years of cable-in-conduit conductors: 1975–1995. J Fus Energ, 1995, 14: 3–12
2 Seeber B. Hand Book of Applied Superconductivity. London: Institute of Physics Publication, 1998. 265–280
3 Yan L G. Recent progress of superconducting magnet technology in China. IEEE Trans Appl Supercond, 2010, 20: 123–134
4 Ciazynski D. Review of Nb3Sn conductors for ITER. Fus Eng Des, 2007, 82: 488–497
5 Liu B, Wu Y, Liu F, et al. Axial strain characterization of the Nb3Sn strand used for China's TF conductor. Fus Eng Des, 2011, 86: 1–4
6 Liu F, Weng P D, Wu Y, et al. Study on the performance test of superconducting strand Nb3Sn (in Chinese). Chin J Low Temp Phys, 2007, 29: 68–72
7 Zhang P X, Liang M, Tang X D, et al. Strain influence on Jc behavior of Nb3Sn multifilamentary strands fabricated by internal tin process for ITER. Physica C, 2008, 46: 1843–1846
8 Liang M, Zhang P X, Tang X D. Strain effect on transport properties of Nb_3Sn multifilament strands prepared by internal tin route (in Chinese). Acta Metallurg Sin, 2009, 45: 223–226
9 Cheng J S, Wang Q L, Dai Y M. Characterization and analysis of microstructures of Nb_3Sn multifilamentary superconductors during diffusion treatment by bronze route (in Chinese). Rare Metal Mat Eng, 2008, 37: 189–192
10 Bruzzone P. AC losses and stability on large cable-in-conduit superconductors. Physica C, 1998, 310: 240–246
11 Fang J, Weng P D, Chen Z M, et al. The ac losses measurement and analysis of superconducting NbTi CICC for HT–7U superconducting Tokamak. Plasm Sci Technol, 2003, 14: 76–82
12 Wang Q L. High Magnetic Field Superconducting Magnet Science (in Chinese). Beijing: Science Press, 2008. 248–299
13 Bottura L, Bruzzone P, Lister J B, et al. Computation of ac losses in the ITER magnets during fast field transients. IEEE Trans Appl Supercond, 2007, 17: 2438–2441
14 Egorov S. AC coupling losses in superconducting multistage cables with and without additional co-twisted copper strands. Physica C, 1998, 310: 272–276
15 Jiang H W, Wu S T. Research of simulation design for CICC based on energy margin and temperature margin. IEEE Trans Appl Supercond, 2010, 20: 1436–1439
16 Jiang H W, Wu S T, Cheng J S. Optimization model of a structural simulation design for a CICC. Chinese Sci Bull, 2011, 56: 2978–2983
17 Li B Z, Bi Y F, Wu W Y. Calculation of ac Losses in large scale superconducting cable (in Chinese). Cryogenics & Superconductivity, 2000, 28: 14–18
18 Fang J. The theoretical and experimental research on HT-7U CICC stability (in Chinese). Doctoral Dissertation. Hefei: Institute of Plasma Physics, CAS, 2002. 58–69
19 Marinucci C, Bottura L, Calvi. A parametric ac loss model of the ITER coils for control optimization. Cryogenics, 2010, 50: 187–199
20 Jiang H W, Wu S T. Research of simulation design model for CICC based on strain (in Chinese). Acta Electronica Sinica, 2010, 38: 1334–1338
21 Wang Y S, Guan X J, Zhang H Y, et al. Progress in inhomogeneity of critical current and index n value measurements on HTS tapes using contact-free method. Sci China Tech Sci, 2010, 53: 2239–2246